596

Generating ~90 nanometer features using near-field contact-mode photolithography with an elastomeric phase mask

John A. Rogers, Kateri E. Paul, Rebecca J. Jackman, and George M. Whitesides[a)]
Department of Chemistry and Chemical Biology, Harvard University, Cambridge, Massachusetts 02138

(Received 3 January 1997; accepted 17 October 1997)

This article describes a near-field photolithographic method that uses an elastomeric phase mask in conformal contact with photoresist. The method is capable of generating ~90 nm lines in commercially available photoresist, using broadband, incoherent light with wavelengths between 330 and 460 nm. Transfer of these patterns into silicon dioxide and gold demonstrates the integrity of the patterned resist. © *1998 American Vacuum Society.* [S0734-211X(98)01201-3]

I. INTRODUCTION

The resolution of standard photolithographic techniques is increased by using masks that manipulate the phase as well as the amplitude of the light used for exposure.[1,2] In one particular method—the phase-edge method[3,4]—a transparent mask induces abrupt changes of the phase of the light used for exposure, and causes optical attenuation at those locations. These phase masks, in conjunction with monochromatic light and a system of imaging optics, can produce features in photoresist as small as ~130 nm when 365 nm light is used for the exposure,[4] and ~100 nm when 248 nm light is used.[2]

In this report, we describe a method for producing ~90 nm features in photoresist using a conformal, contact phase mask and incoherent, polychromatic ultraviolet (uv) light with wavelengths between 330 and 460 nm. Compared to other phase-shifting photolithographic techniques, this method has four major advantages. It is very simple and inexpensive, and allows features with sizes on the order of 100 nm to be produced from masks with features having sizes on the order of microns. The mechanical flexibility of the mask eliminates problems in alignment of mask and surface, and allows patterning of surfaces with significant topography. Mechanical compression and extension of the mask allows for adjustment of the in-plane and out-of-plane features on its surface. Most importantly, with conformal contact between the resist and the mask, the resolution is determined by the wavelength of the light used for exposure *in the photoresist.* For a given source of light, reduction of the wavelength in the resist can be achieved by increasing the index of refraction of the resist. We note that this property was recognized first in early work using conformable amplitude masks made from thin, flexible glass, where it was demonstrated that ~400 nm lines in photoresist could be produced using broadband light (436, 405, and 365 nm) from a mecury lamp.[5,6]

The disadvantages of performing near-field lithography with an elastomeric phase mask include the difficulty of achieving accurate registration with a flexible mask, and uncertainties (on the order of 1 μm over a 1 mm pattern) in the distances between features. Also, because this technique involves 1:1 imaging, production of nanometer features that are separated by nanometers requires features with similar sizes on the mask. For these reasons, we believe that this method is currently best suited for generating single-level structures, where local linewidths are important, but accurate distances between separated features in the pattern are not.

We begin this article with a qualitative description of the

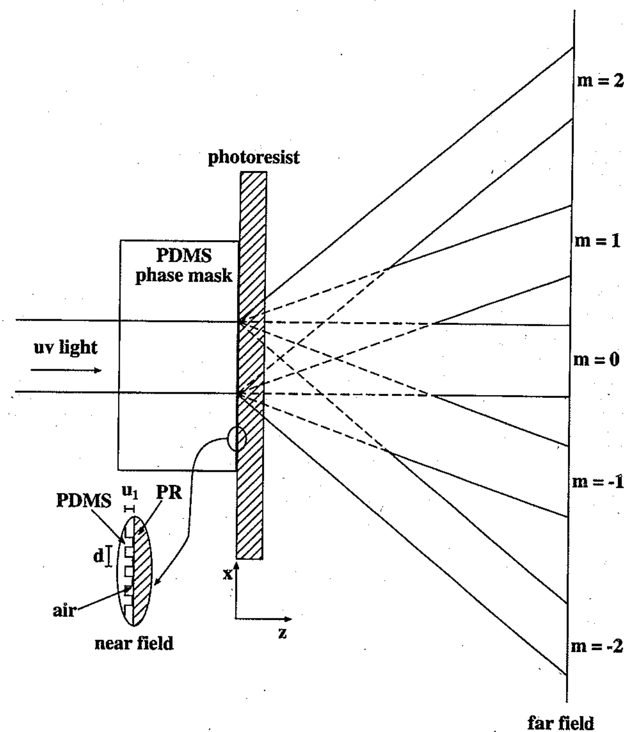

FIG. 1. Geometry of the elastomeric phase mask, the photoresist, the light used for exposure, and qualitative definitions of the near and far fields. The phase of light passing through the mask is modulated according to the wavelength of the light, the surface relief of the mask, and the difference between the index of refraction of the air and the mask. Modulations of the phase create modulations in the intensity in the near field, and diffracted orders in the far field.

[a)]Electronic mail: gwhitesides@gmwgroup.harvard.edu

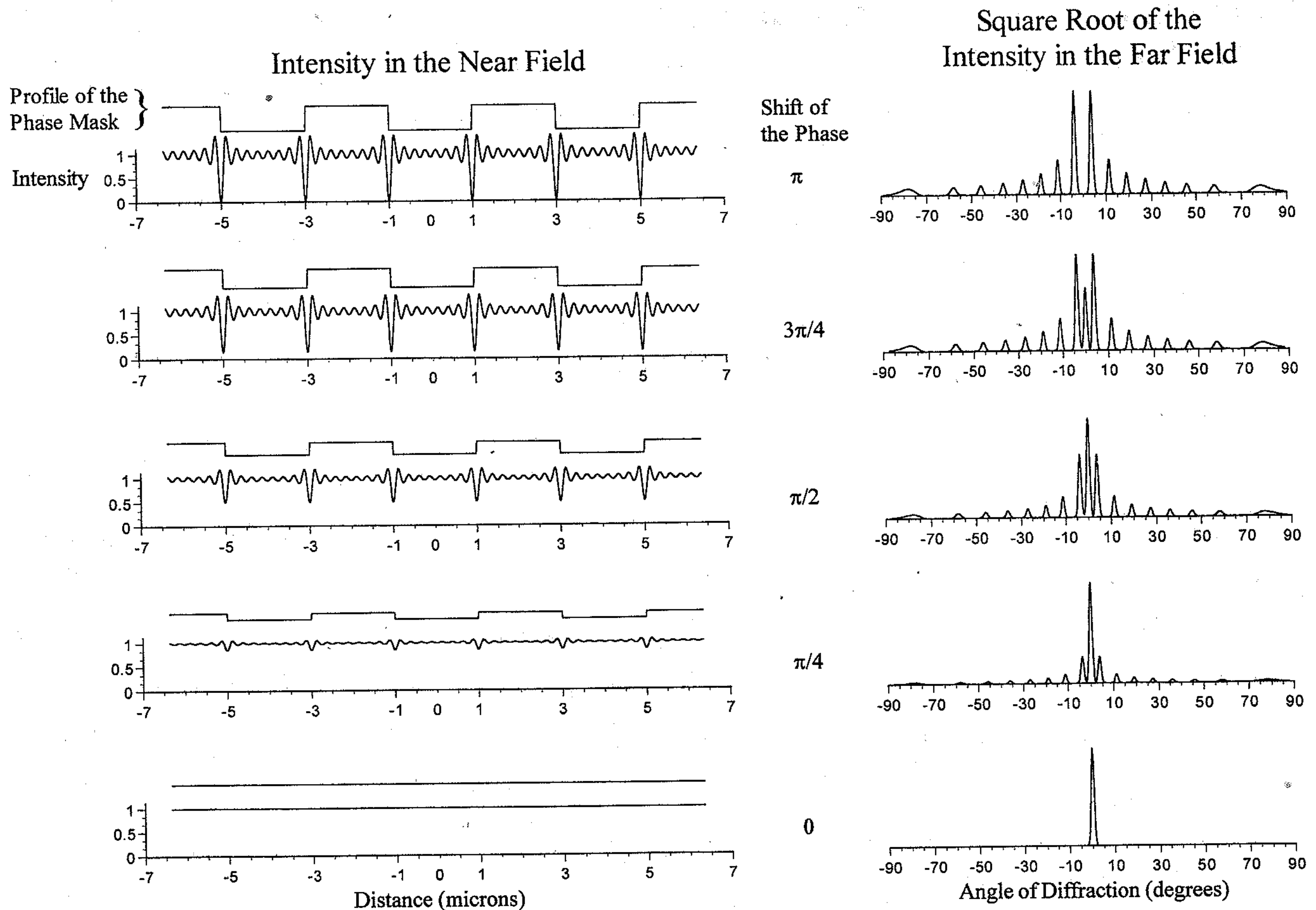

FIG. 2. Variation of the near- and far-field patterns of intensity as the depth of modulation of the phase induced by the mask varies between π and 0. As the phase changes from π to 0, the depth of modulation of the intensity in the near field decreases. This corresponds to an increase in the intensity of the zeroth order diffracted beam in the far field. For these calculations, the wavelength of the light used for exposure was 365 nm, and the index of refraction of the photoresist was 1.4. (We display the square root of the intensity in the far field in this figure in order to highlight the structure of the pattern of diffraction. For each plot, the intensities are scaled to the largest peak.)

procedure, and follow with an analysis of the pattern of intensity in the near field. We illustrate the procedure for fabricating the elastomeric phase mask, and present data collected with an optical microscope used in transmission mode that elucidates the mechanism for generating contrast with these masks. We then describe the means for exposing the photoresist through the masks, and we present and analyze the structures produced in the photoresist. Finally, we demonstrate these patterns in photoresist can be transferred to the substrate using reactive ion etching and to thin metal layers using a standard liftoff procedure.

II. THEORY

A. General considerations

Consider light passing through a transparent mask (Figure 1). The phase, $\varphi(x)$, of light with wavelength λ that emerges from the mask is related to the relief of the surface of the mask, $u(x)$, and to the difference between its index of refraction and that of the surroundings, Δn, by Eq. (1). If we neglect the finite thickness of the relief on the surface of the mask, the electric field just after emerging from the mask (at position $z=0^+$) can be related to the electric field just before emerging from the mask (at position $z=0^-$) by Eq. (2):

$$\varphi(x)=\frac{2\pi}{\lambda}\Delta n u(x), \tag{1}$$

$$\begin{aligned}E(x,z=0^+)&=E(x,z=0^-)\exp[i\varphi(x)]\\&\equiv E(x,z=0^-)\tau(x).\end{aligned} \tag{2}$$

Equation (2) defines the transmission function of the phase mask, $\tau(x)$.

When the relief of the surface is binary and has magnitude u_1 and periodicity d, then $\tau(x)$ can be described by Eq. (3).

$$\tau(x)=\begin{cases}\exp\left(\frac{2\pi i}{\lambda}u_1\Delta n\right) & md<x<\left(m+\frac{1}{2}\right)d, \quad m=\dots-2,-1,0,1,2\dots\\ 1 & \text{otherwise.}\end{cases} \tag{3}$$

When $u_1=\lambda/(2\Delta n)$, the phase shift is equal to π, and the electric field undergoes abrupt changes in sign at the edges where the phase shift occurs. Since the electric field is continuous in the photoresist, these changes in sign induce nulls in the intensity near the surface of the mask. This effect is the basis for generating contrast with masks that manipulate only the phase of the light.

B. Quantitative analysis

Although this qualitative description accounts for the presence of the nulls, a more detailed analysis is necessary to determine the distribution of intensity. Here we outline a very simple scalar analysis that captures most of the salient aspects of this problem. The calculations are similar to those presented previously for proximity and projection photolithography with phase masks,[1–4,7] but is appropriate for the case when the phase mask is in conformal contact with the photoresist. It is based on the generalized Abbe theory for image formation.[8–10]

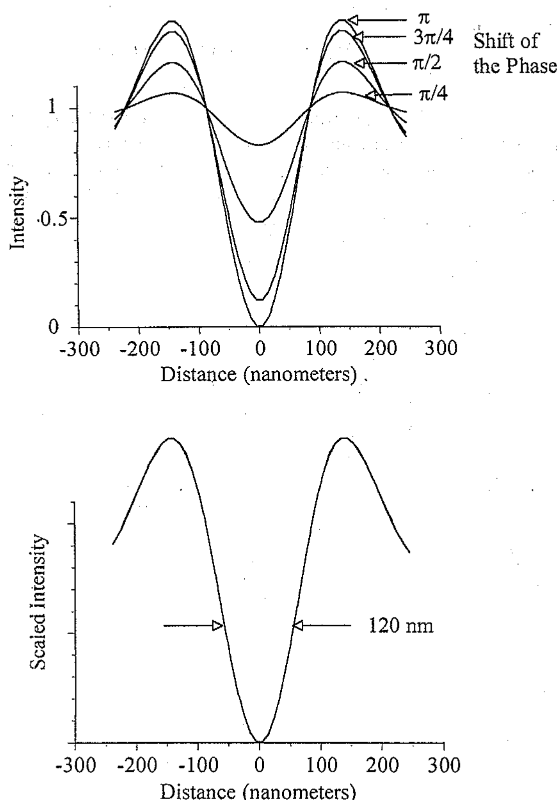

FIG. 3. Variation of the pattern of intensity in the near-field near a minimum as a function of the shift of the phase. The upper frame shows that the depth of the minimum decreases as the phase deviates from π. The lower frame shows scaled patterns of intensity in the same region as the upper frame. The lower frame shows the dips in intensity for each of the shifts of the phase. The intensities were linearly scaled to have the same minima and maxima. For these computations, the wavelength of the light used for exposure was 365 nm, and the index of refraction of the photoresist was 1.4.

In the Fraunhofer regime, Fourier transformation of the transmission function, $\tau(x)$, yields the far field diffraction pattern. For a mask with periodicity d, diffracted orders in the far field appear at angular locations defined by Eq. (4).

$$\sin(\theta_m)=\frac{m}{d}\cdot\left(\frac{\lambda}{n}\right), \quad m=\dots-2,-1,0,1,2,\dots . \tag{4}$$

In this equation, the index of refraction of the material into which the light passes as it emerges from the mask is n, and λ is the wavelength of the light in vacuum. The order of the diffraction is m. To compute the near field pattern of intensity, we define an aperture that removes the evanescent waves ($|m|\lambda/(nd)>1$) and admits only the light propagating out of the mask. Fourier transformation of this filtered pattern of diffraction defines the electric field near the surface of the mask. We used this procedure to compute the patterns of intensity for shifts of the phase between zero and π, for masks with different periodicities, for illumination with light of different wavelengths, and for photoresist with different indices of refraction. (For these computations, we held fixed the ratio of the width of the illuminating beam to the wavelength of light and the periodicity of the grating.) While some of these effects are related, it is instructive to consider them separately.

Figure 2 illustrates the patterns of intensity in the near and far fields for binary phase masks that induce shifts of the phase between 0 and π. As the phase deviates from π, the amount of light that appears in the zeroth order in the far field increases. This increase corresponds to a reduction in the contrast in the near field. As Figure 3 illustrates, the widths of the dips in intensity do not change with changes in the shift of the phase.

Figure 4 illustrates the near- and far-field intensity patterns produced by binary phase masks that induce shifts of the phase equal to π, but have different periodicities. As the periodicity of the mask decreases, fewer diffracted orders are produced. This reduction in diffracted orders corresponds to a reduction in the structure present in the near-field pattern. When only two diffracted beams appear, the near-field pattern simplifies to a single sinusoid whose periodicity matches the periodicity of the mask. (This effect has been used in the past to generate holographic gratings with periodicities between 0.2 and 1.5 μm in optical fibers[11,12] and on surfaces.[13–15]) As Figure 5 illustrates, there is little variation in the width of the dips in the intensity with the periodicity

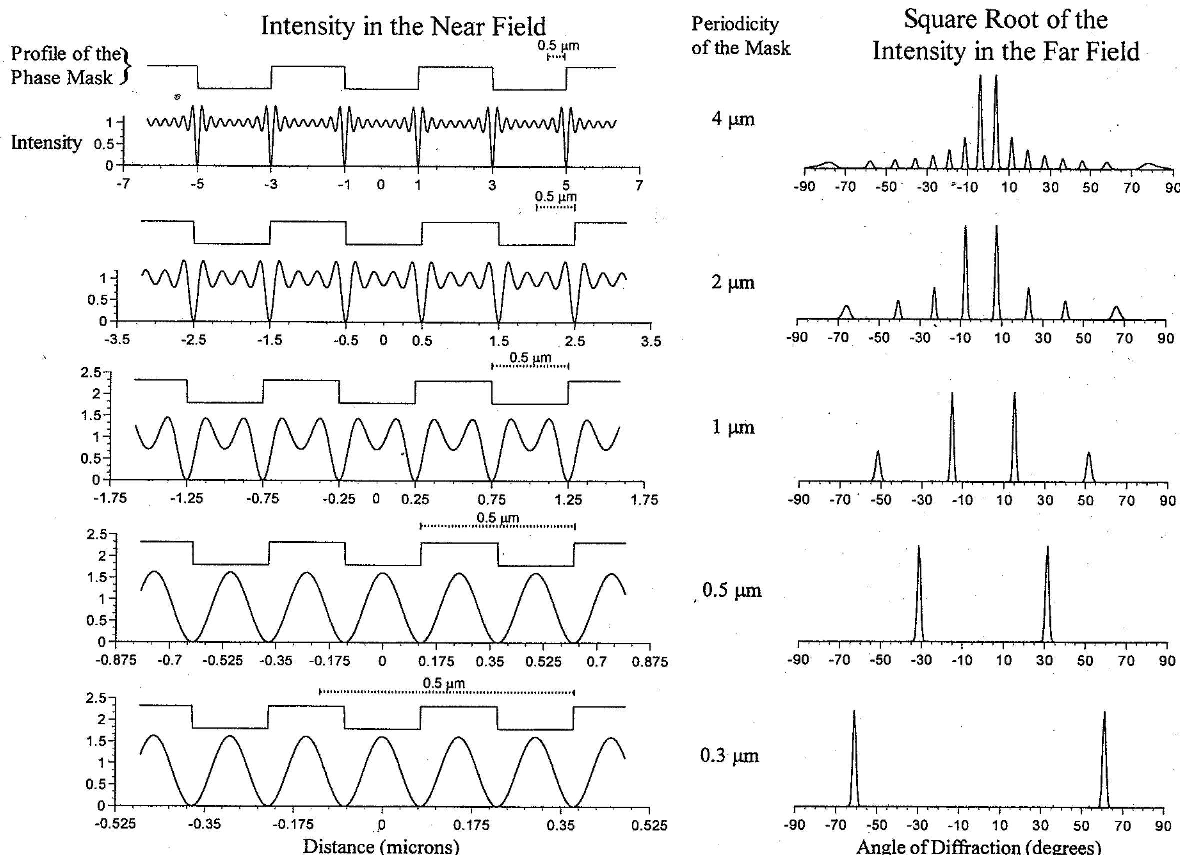

FIG. 4. Variation of the near- and far-field patterns of intensity as the periodicity of the mask changes. As the periodicity decreases, fewer diffracted orders emerge from the mask. This reduction in the number of diffracted orders corresponds to a reduction in the structure of the pattern of intensity in the near field. When only the first order beams emerge a simple sinusoidal pattern of intensity whose period matches that of the mask results. For these computations, the wavelength of the light used for exposure was 365 nm, and the index of refraction of the photoresist was 1.4. (We display the square root of the intensity in the far field in this figure in order to highlight the structure of the pattern of diffraction. For each plot, the intensities are scaled to the largest peak.)

of the mask provided that several diffracted orders emerge. When only the first order beams appear, the widths decrease as the periodicity of the mask decreases until the first order beams become evanescent.

For a phase mask with a given periodicity, the number of diffracted orders that emerges increases as the wavelength of the exposure light in the photoresist decreases. Increasing the number of diffracted orders increases the resolution. To illustrate this effect, Figure 6 shows near and far field diffraction patterns formed by passing light with different wavelengths through a phase mask that induces shifts of the phase equal to π. Figure 7 shows that in the near field, the dips in the intensity get narrower as the wavelength in the photoresist decreases. In the special case in which the same number of diffracted orders appear from the phase mask when the wavelength of the light used for exposure is changed (for example, if only the first order beams appear), then the near-field patterns of intensity remain the same.

The reduction in wavelength necessary to increase the resolution can be achieved by (1) reducing the wavelength of the source of light or (2) increasing the index of refraction of the photoresist. This second possibility is not present in standard phase-shifting photolithographic methods, and may pro-

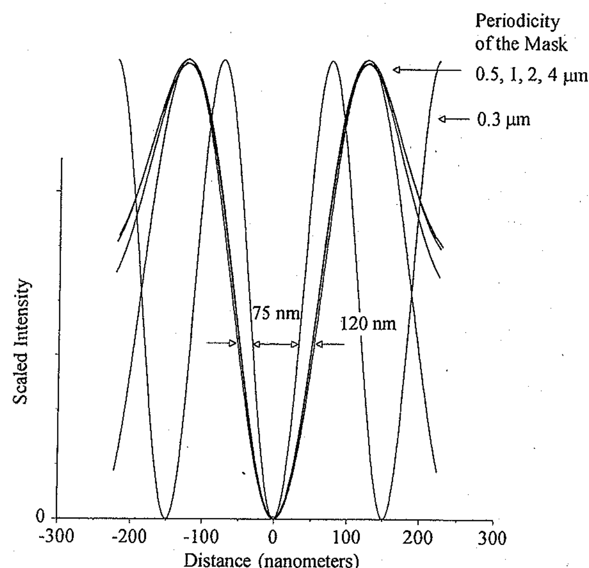

FIG. 5. Comparison of the near-field patterns of intensity in the region of a minimum in intensity as a function of the periodicity of the mask. (The intensities were normalized.) The widths of the dips in intensity are insensitive to the periodicity of the mask until only the first order diffracted beams appear. For these computations, the wavelength of the light used for exposure was 365 nm, and the index of refraction of the photoresist was 1.4.

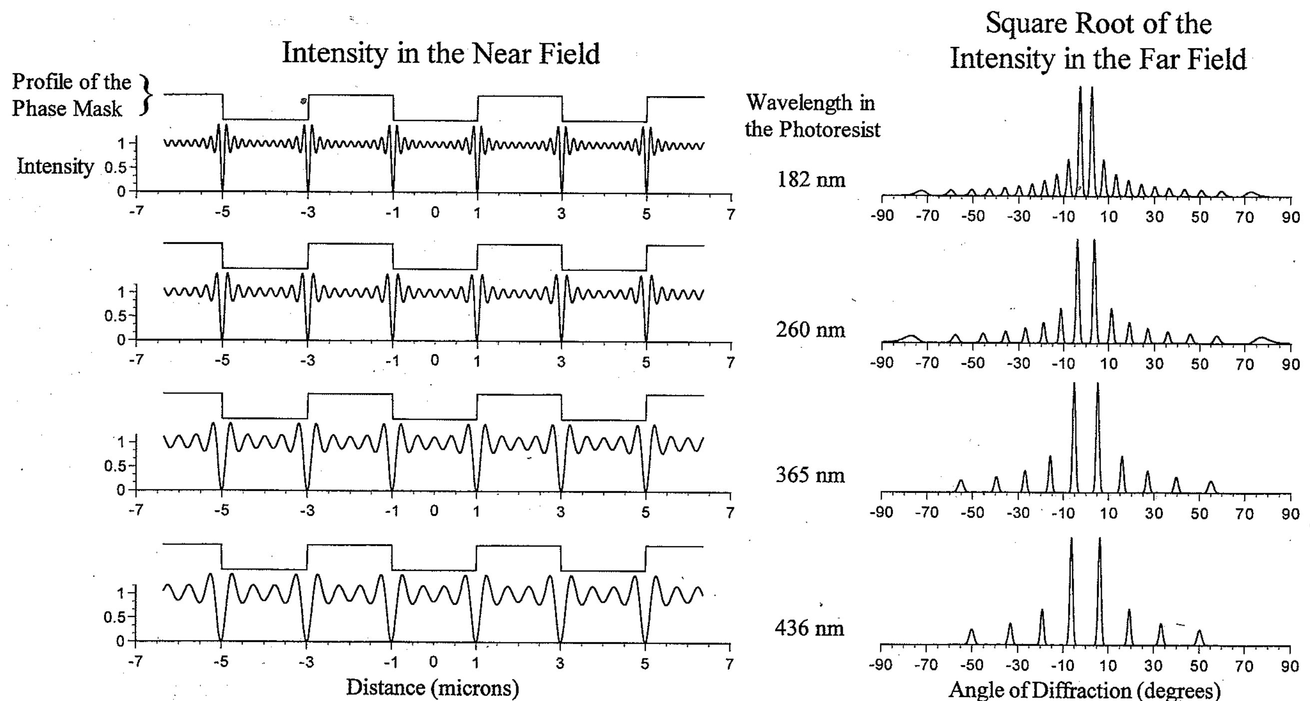

FIG. 6. Variation of the near- and far-field patterns of intensity as the wavelength of the light in the photoresist changes. As the wavelength decreases, more diffracted orders appear from the mask. This increase in diffracted orders corresponds to the addition of higher spatial frequencies in the near field. The wavelength can be decreased by either changing the source of light, or by changing the index of refraction of the photoresist. 440 nm and 365 nm light are emitted by mercury lamps. The wavelength of 365 nm light in photoresist with index of refraction 1.4 is 260 nm. The wavelength of 365 nm light in photoresist with index of refraction 2.0 is 180 nm. (We display the square root of the intensity in the far field in this figure in order to highlight the structure of the pattern of diffraction. For each plot, the intensities are scaled to the largest peak.)

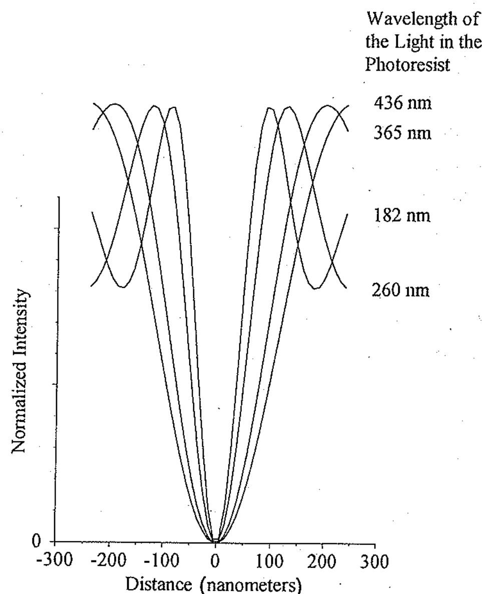

FIG. 7. Comparison of the near-field patterns of intensity in the region of a minimum in intensity as a function of the wavelength of the light used for exposure evaluated in the photoresist. The widths of the dips in intensity decrease as the wavelength decreases: 440 nm and 365 nm light are emitted by mercury lamps; 260 nm is the wavelength of 365 nm light in photoresist with index of refraction 1.4; 182 nm is the wavelength of 365 nm light in photoresist with index of refraction 2.0.

vide an avenue for increasing photolithographic resolution without changing the wavelength of the source of light. As an illustration, if 365 nm light is used to expose photoresist with index of refraction ~1.4, lines as narrow as $\sim 365/(1.4\times 4)=65$ nm can, in principle, be produced with the method described here. If there is a gap of air between the mask and the resist that is wider than the decay length of the evanescent waves at the surface of the mask, then only $\sim 365/4=90$ nm lines are possible. This difference in width occurs because the photoresist that is in contact with the mask causes some diffracted orders that would otherwise be evanescent to pass through the mask and into the photoresist. We note that the presence of the air gaps between recessed regions of the mask and the photoresist may decrease the value of n that appears in Eq. (4). Calculations and experiments to investigate the effects of the air gaps and the index of the photoresist on the patterns of intensity in the near field of the mask are the subject of current work.

We note that, for simplicity, the discussion given above focuses on the behavior of light passing through periodic square-wave masks. Most of the conclusions, however, can be extended to aperiodic structures. This extension is possible because the dips in the intensity at phase-shifting boundaries result from local effects (i.e., within an optical wavelength). Figure 8 illustrates the intensities in the near

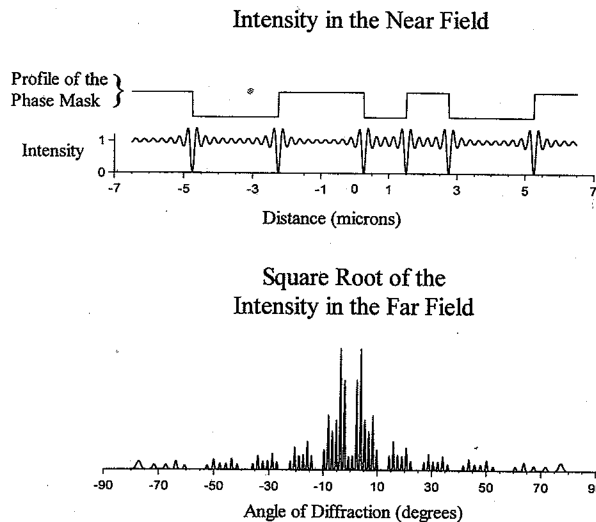

FIG. 8. Near- and far-field patterns of intensity for a binary aperiodic phase mask that modulates the phase by π. The results indicate that the dips in intensity at the phase-shifting boundaries are independent of the positions of other boundaries (provided that their separation is greater than approximately one optical wavelength).

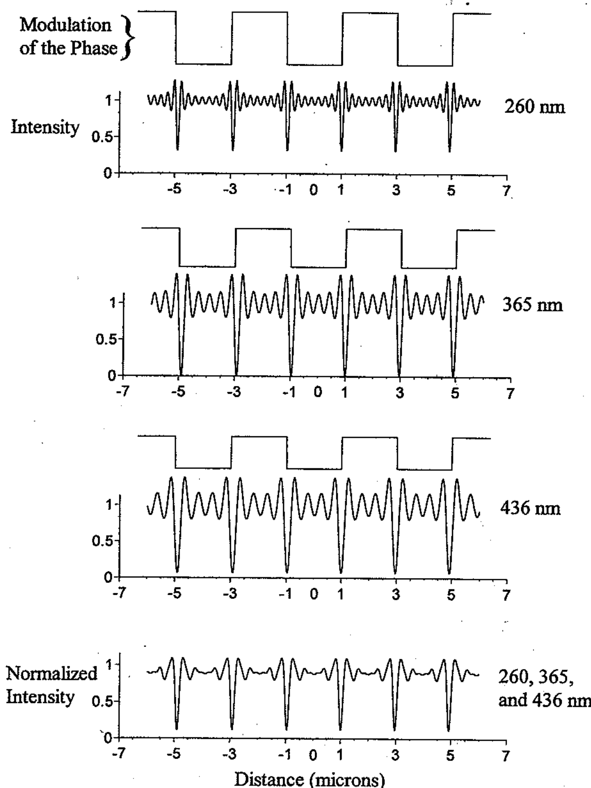

FIG. 9. Variation of the intensity in the near field of a binary phase mask for monochromatic light of different wavelengths and for polychromatic light. The phase mask induces a shift of the phase of π for 365 nm light, and has an index of refraction that is independent of wavelength between 260 and 435 nm. These results show that the effects of multiple wavelengths are to reduce the variations in the intensity between phase shifting boundaries and to reduce the contrast.

and the far fields produced by passing light through an aperiodic binary mask.

We conclude this section by reviewing the approximations associated with the calculations. First, the simulations used monochromatic light, and did not include the finite spatial and temporal coherence of the light used for the exposure. Polychromatic light reduces the amplitude of oscillations in the intensity in the near field that occur between phase shifting boundaries (Figure 9). We also did not account for reflections at the interface between the photoresist and the substrate, or at the interfaces between the mask and the air, and the mask and the photoresist. In addition, we used all of the approximations associated with the Fraunhofer theory and we neglected the evanescent waves. In spite of these limitations, the results qualitatively correspond well with experimental observations described below.

III. EXPERIMENTAL PROCEDURES

We fabricated a set of elastomeric phase masks by casting and curing polydimethylsiloxane (PDMS) prepolymer (Dow Corning Sylgard 184) against masters consisting of patterned lines of photoresist (Shipley 1805) prepared by conventional photolithography (Figure 10).[16] The depth of surface relief of the phase masks was varied by changing the thickness of the photoresist. The total thickness of the masks was ~5 mm; the Young's modulus was on the order of a few MPa. Using masks with depths of surface relief between 430 and 510 nm, we determined the phase shifts for each mask at 514 nm (argon ion laser) and 355 nm (tripled YAG laser) from the pattern of intensity in the far field (i.e., the ratio of the intensity of the zeroth order beam to the intensity of the first order beam) (Figure 11). Using gratings with depths of surface relief between 0.1 and 1.40 μm, and the index of refraction of PDMS determined from the data illustrated in Figure 11, we measured the patterns of intensity at the surface of the phase mask as a function of modulation of the phase. We performed this measurement by focusing a microscope on the surfaces of the gratings and using green light for illumination. A CCD camera was used to digitize the images (Figures 12 and 13). As expected from the theory section, results illustrated in Figures 12 and 13 indicate that masks that shift the phase by $\sim\pi$ provide the greatest contrast in intensity at the surface of the mask.

Using a set of elastomeric phase masks that produce shifts of the phase approximately equal to π for wavelengths emitted by a mercury lamp (i.e., depths between 400 and 500 nm), we generated structures in photoresist (Shipley 1805). We first allowed the elastomeric phase mask to come into conformal contact with the photoresist, and then we exposed the resist through the phase mask using a standard mask aligner (Karl Suss MJB3 UV400) equipped with a mercury lamp (emission peaks at 365, 405, and 436 nm) for between 0.25 and 2.5 s. A 1:5 dilution of Shipley's Microposit 351 into water was used to develop the exposed photoresist. Development times between 30 and 90 s were used.

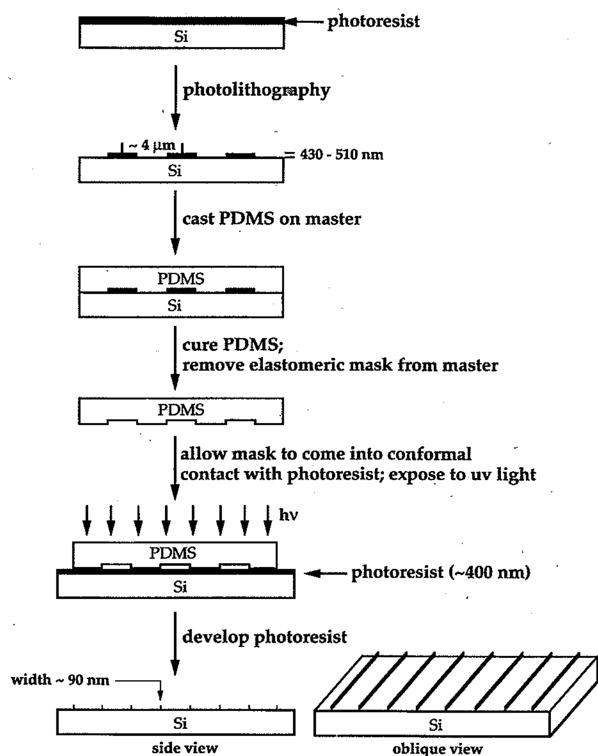

FIG. 10. Schematic illustration of the fabrication of nanometer-sized structures by near-field contact-mode photolithography. Casting and curing a prepolymer of polydimethylsiloxane (PDMS) on a master, generated by photolithography, forms an elastomeric phase shift mask. The mask is allowed to come into conformal contact with a layer of photoresist (~400 nm thick) supported by a silicon wafer. Exposure of the photoresist to collimated, broadband ultraviolet light through the mask and subsequent development of the photoresist produces structures with widths on the order of 100 nm.

In order to demonstrate the integrity of the structures in photoresist, we transferred the patterns into gold (500 Å; using Cr as an adhesion promoter) using a standard liftoff procedure, and into silicon dioxide (1200 Å) by anisotropic etching using reactive ion etching with a plasma of CF_4.

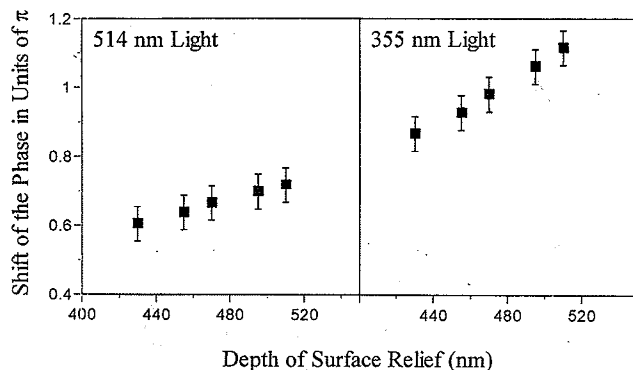

FIG. 11. Shift in the phase induced by phase masks with different depths of surface relief for 514 nm light (argon ion) and 355 nm light (tripled Nd:YAG). The phase was computed from the depth of surface relief and the pattern of intensity in the far field (i.e., the ratio of the intensity of the zeroth to the first order diffracted beams). These measurements indicate the range of shifts of the phase that these masks will induce in light emitted from a mercury lamp (330–460 nm).

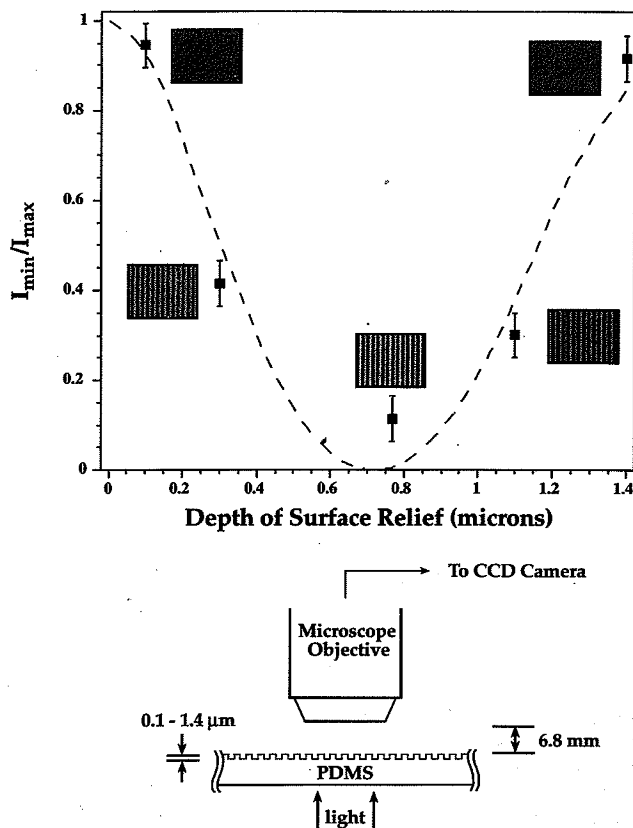

FIG. 12. Computed (solid line) and measured (symbols) ratios of the minimum intensity to the maximum intensity at the surface of phase masks with different depths of surface relief. Measurements were performed with an optical microscope using green light for illumination and a CCD camera. (Images are shown as insets, and a schematic illustration of the experiment is shown in the lower frame.) The computations used procedures described in the theory section. For the results illustrated here, we assumed that the masks deviated from a perfectly square-wave shape by an amount (~50 nm) consistent with scanning electron micrographs of the lines of photoresist used for fabricating the masks.

IV. RESULTS AND DISCUSSION

We have generated patterns of photoresist using phase masks with patterns consisting of arrays of parallel lines (Figures 14 and 15) and more complex shapes (Figure 16). In all cases, the lines had widths of ~90 nm; this resolution is a factor of six better than the specifications for the mask aligner under optimal conditions when a conventional amplitude mask is used. We also generated dots with nanometer dimensions by exposing photoresist twice with a periodic binary phase mask, rotating the mask by ninety degrees between exposures (Figure 17). Figure 18 illustrates that the patterns of photoresist can be transferred into gold using standard liftoff techniques, and into SiO_2 using reactive ion etching. (We note that it is possible to use the same experimental procedures with image reversal photoresist to generate "negatives" of structures illustrated in Figures 14–18.)

The experimental results correspond well with the theory. Figures 12 and 13 show that measured and calculated pat-

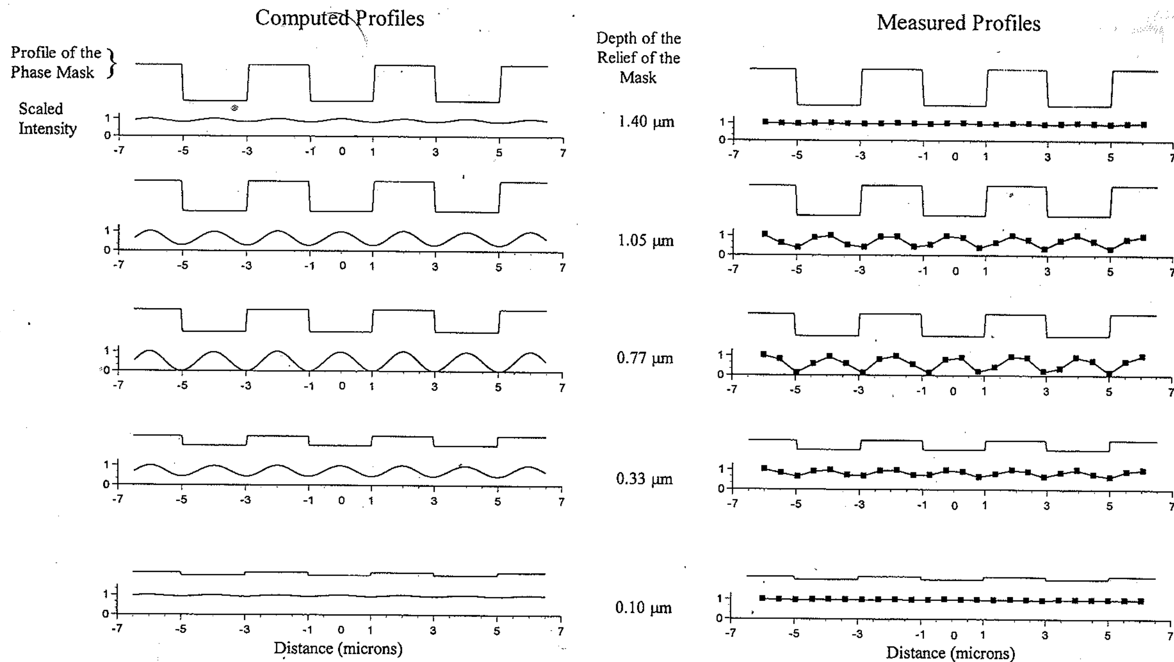

FIG. 13. Computed and measured patterns of intensity at the surfaces of phase masks with depths of surface relief between 0.1 and 1.40 μm. The measurements were performed with an optical microscope using green light for illumination and a CCD camera. The computations used procedures described in the theory section. For the results illustrated here, we assumed that the masks deviated from a perfectly square-wave shape by an amount (~50 nm) consistent with scanning electron micrographs of the lines of photoresist used for fabricating the masks. We used the numerical aperture (0.6) specified by the manufacturer of our microscope objective (Leitz Wetzlar, 567005).

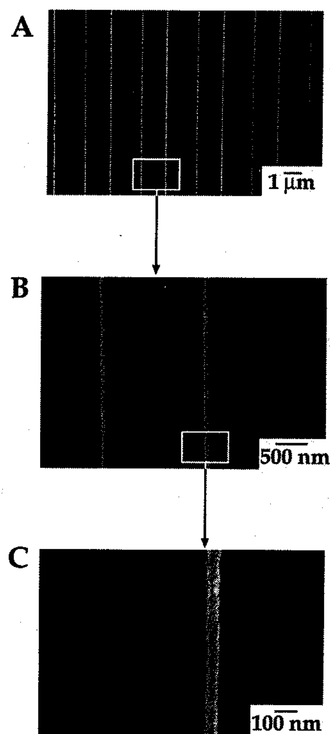

FIG. 14. Scanning electron micrographs (SEMs) of lines of photoresist (~100 nm) formed by near-field contact-mode photolithography using an elastomeric phase mask with relief structure consisting of parallel lines (2 μm spaced by 2 μm). These images illustrate many (A), uniform, straight lines (B) with widths on the order of 100 nm (C). Light regions correspond to photoresist and dark regions correspond to SiO_2/Si.

terns of intensity at the surfaces of phase masks with different depths of surface relief are in good agreement, indicating that shifts of the phase provide the primary mechanism for generating contrast in the near field. The photolithography supports this conclusion. For example, we detected no dependence of the width of the lines in the photoresist on the depth of surface relief of the phase mask. This observation is supported by results illustrated in Figure 3. In addition, com-

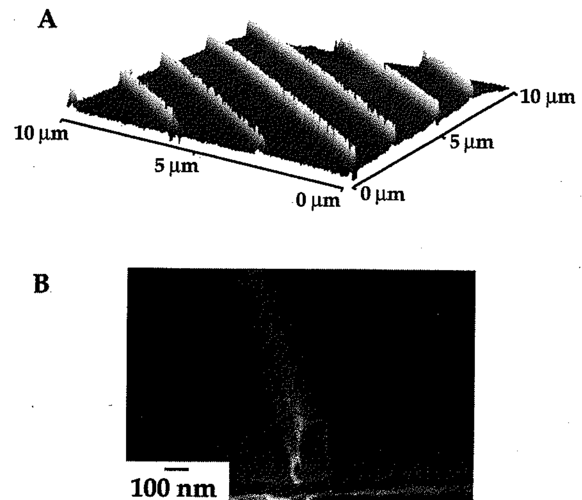

FIG. 15. Parallel lines formed in photoresist using nearfield contact-mode photolithography have widths on the order of 100 nm and are ~300 nm in height as imaged by (A) AFM and by (B) SEM.

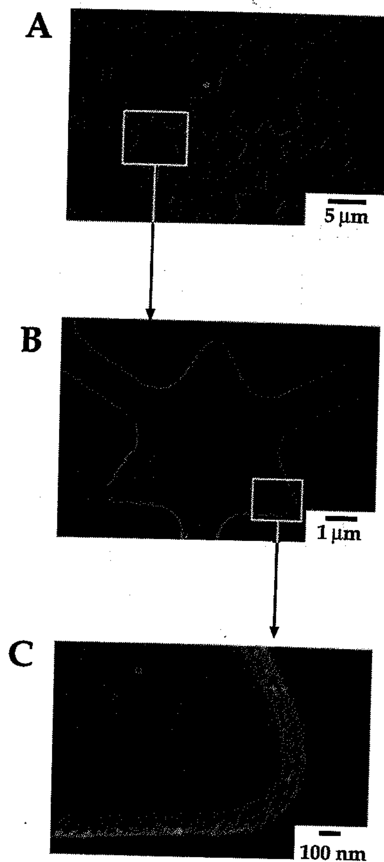

FIG. 16. Scanning electron micrographs (SEMs) of patterns of photoresist (~100 nm) formed by near-field contact-mode photolithography using an elastomeric phase mask with relief structure consisting of an array of connected triangles (5 μm diameter). These images illustrate large collections (A) of uniform lines (B) with widths on the order of 100 nm (C). Light regions correspond to photoresist and dark regions correspond to SiO_2/Si.

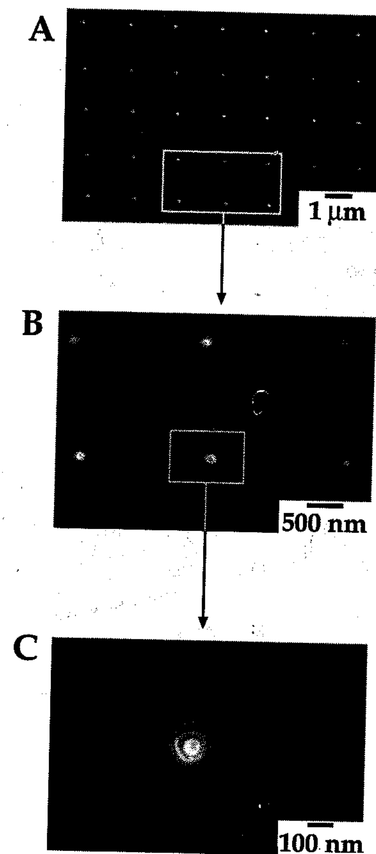

FIG. 17. Scanning electron micrographs (SEMs) of dots in photoresist formed by near-field contact-mode lithography using an elastomeric phase mask with relief structure consisting of parallel lines (2 μm) spaced by 2 μm. The dots were formed by exposing the photoresist through this mask, rotating the mask by 90 degrees, and then exposing the resist again. The images illustrate large defect-free areas (A), and generation of uniform features (B) with diameters on the order of 100 nm (C). Light regions correspond to photoresist and dark regions correspond to SiO_2/Si.

putations show that the widths of dips in the intensity are not sensitive to the geometry of the mask (Figures 5 and 8). Experimental data presented in Figures 14 and 16 support this result.

Finally, we observed that the optimal time for exposure using the method described here was significantly shorter than the exposure time for resist exposed through a conventional amplitude mask (1.0 s compared to 5.5 s). We believe that the difference arises because the phase shift is never precisely π for all wavelengths of exposure, resulting in nonzero intensity at the minima and partial exposure of the photoresist in these regions (Figure 9). We found that the time for exposure did not significantly affect the width of the lines provided it was between 0.25 and 2.5 s, and that the time for developing was properly adjusted.

V. CONCLUSIONS

The lithographic method described in this article offers many advantages relative to other techniques. Lines with ~90 nm width can be produced over large areas with incoherent, broadband light. Since no optics are required for projection, large areas can be patterned in a single exposure, and there is no uncertainty associated with positioning the resist precisely at the image plane. In addition, fabrication of the elastomeric phase masks is easy, and is low cost.

Contact mode lithography with elastomeric phase masks has a resolution that is determined not only by the wavelength of the light used for exposure, but also by the index of refraction of the photoresist. Increasing the index of the photoresist may provide a route to increasing the resolution of photolithography that is more promising than decreasing the wavelength of the exposure light, particularly in light of difficulties associated with generating, focusing, and manipulating deep-ultraviolet and x-ray radiation.

Future work includes experimental determination of the relationship between the resolution and the index of the photoresist. Also, we will assess the dimensional stability of these flexible masks, both during long-term use of a single mask, and during generation of multilayer structures.

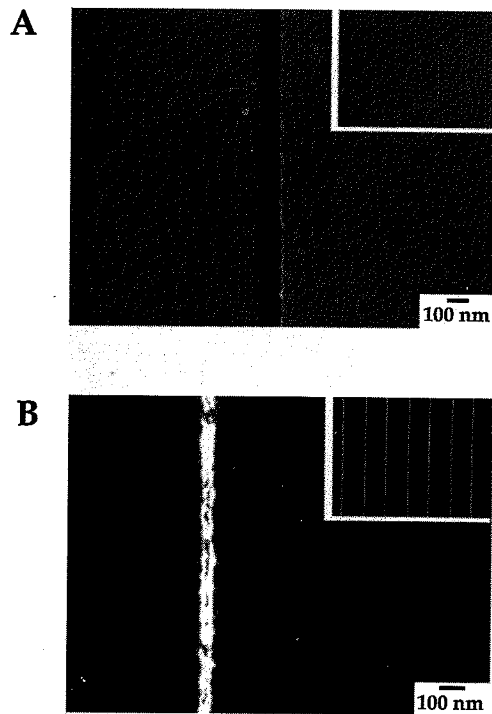

FIG. 18. Scanning electron micrographs (SEMs) of lines formed by near-field contact mode lithography and subsequent treatment. (A) Patterns in photoresist transferred into gold by standard liftoff procedures. The line width is ~90 nm. Light areas correspond to gold, and dark areas correspond to silicon. (B) Patterns in photoresist transferred into silicon dioxide on silicon by reactive ion etching with a plasma of CF_4.

ACKNOWLEDGMENTS

This research was supported in part by the National Science Foundation (PHY-9312572), ONR and DARPA, and by the William F. Milton Fund of the Harvard Medical School. It also used MRSEC Shared Facilities supported by the NSF under Award No. DMR-9400396. One of the authors (J.A.R.) gratefully acknowledges funding from the Harvard University Society of Fellows, and R.J.J. gratefully acknowledges a scholarship from NSERC.

[1]M. Levenson, *Physics Today*, 28 (1993).
[2]J. C. Langston and G. T. Dao, Solid State Technol. 57 (1995).
[3]K. H. Toh, G. Dao, R. Singh, and H. Gaw, SPIE **1496**, 10th Annual Symposium on Microlithography, 1990, pp. 27–53.
[4]T. Tanaka, S. Uchino, N. Hasegawa, T. Yamanaka, T. Terasawa, and S. Okazaki, Jpn. J. Appl. Phys., Part 1 **30**, 1131 (1991).
[5]H. I. Smith, N. Efremow, and P. L. Kelley, J. Electrochem. Soc. **121**, 1503 (1974).
[6]J. Melngailis, H. I. Smith, and N. Efremow, IEEE Trans. Electron Devices 496 (1975).
[7]P. E. Dyer, R. J. Farley, and R. Geidl, Opt. Commun. **115**, 323 (1995).
[8]M. V. Klein, *Optics* (Wiley, New York, 1970).
[9]J. W. Goodman, *Introduction to Fourier Optics* (McGraw–Hill, New York, 1968).
[10]M. Born and E. Wolf, *Principles of Optics* (Pergamon, New York, 1980).
[11]K. O. Hill, B. Malo, F. Bilodeau, D. C. Johnson, and J. Albert, Appl. Phys. Lett. **62**, 1035 (1993).
[12]B. Malo, D. C. Johnson, F. Bilodeau, J. Albert, and K. O. Hill, Opt. Lett. **18**, 1277 (1993).
[13]D. M. Tennant, T. L. Koch, P. P. Mulgrew, R. P. Gnall, F. Ostermeyer, and J-M. Verdiell, J. Vac. Sci. Technol. B **10**, 2530 (1992).
[14]D. M. Tennant, T. L. Koch, J-M. Verdiell, K. Feder, R. P. Gnall, U. Koren, M. G. Young, B. I. Miller, M. A. Newkirk, and B. Tell, J. Vac. Sci. Technol. B **11**, 2509 (1993).
[15]P. Brock, M. D. Levenson, J. M. Savislan, J. R. Lyerla, J. C. Cheng, and C. V. Podlogar, J. Vac. Sci. Technol. B **9**, 3155 (1991).
[16]A. Kumar and G. M. Whitesides, Appl. Phys. Lett. **63**, 2002 (1993).